International Journal of Research and Review
Vol. 10; Issue: 6; June 2023
Website: www.ijrrjournal.com
Review Paper *E-ISSN: 2349-9788; P-ISSN: 2454-2237*

Wire ARC Additive Manufacturing of Functional Metals - A Review

J. Pradeep Kumar[1], R. Arun Prakash[2], R. Jaanaki Raman[3], N. Jerome Festus[4], M. Kanmani[5], S. Praveen Nath[6]

[1,2,3,4,5,6] Department of Production Engineering, PSG College of Technology, Coimbatore, India

Corresponding Author: J. Pradeep Kumar

DOI: https://doi.org/10.52403/ijrr.20230671

ABSTRACT

The need for wire arc additive manufacturing (WAAM) has substantially expanded in recent years, and it has emerged as a possible alternative to subtractive production. According to research, the mechanical qualities of wire arc additively manufactured materials are comparable to cast material. When compared to other fusion sources, WAAM provides considerable cost savings as well as a higher deposition rate. However, WAAM presents considerable problems, including undesired microstructures and mechanical characteristics, large residual stresses, and deformation. As a result, more study is required to address the aforementioned problems by optimizing process parameters and post-deposition heat treatment. In accordance with the foregoing, this paper attempts to fill the gap by presenting a comprehensive review of WAAM literature, which includes stage-wise development of WAAM, metals, and alloys used, effects of process parameters, and methodologies used by various researchers to improve the quality of WAAM components. Furthermore, this work suggests topics that could be explored further in the future.

Keywords: Wire Arc Additive Manufacturing, Subtractive production, cost saving, optimizing parameters, stage wise development.

1. INTRODUCTION

Metal wire is used as the feedstock material and an arc serves as the heat source in wire arc additive manufacturing. The primary cost of metal wire typically amounts to 10% of the weight of metal powder. The metal wire is heated, melted, and then transported to the melt pool where it solidifies at the melt pool border to create components that were digitally created during the WAAM process. The direct manufacture of intricate thin-walled objects using WAAM, a type of droplet-based additive manufacturing technology, is particularly promising. The fast deposition rate of WAAM makes it ideal for creating large-scale components. The WAAM method for 3D printing metal objects uses an arc welding procedure and is a version of the Direct Energy Deposition technique. Unlike the more popular metal powder AM methods, WAAM melts metal wire utilizing an electric arc as the heat source which is shown in figure 1.1

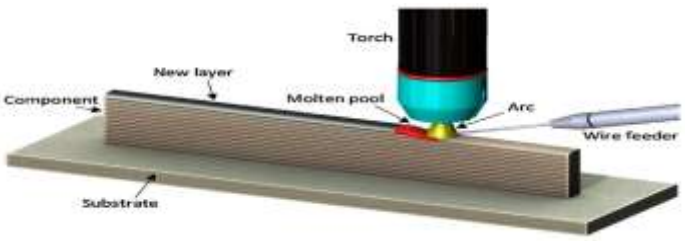

Figure 1.1 Wire arc additive manufacturing process

The robotic arm controls the operation, and the shape is constructed on a substrate material (a base plate) from which the finished object can be cut. When the wire is melted, it is extruded onto the substrate as beads. The beads combine to form a coating of metal as they adhere to one another. After that, the procedure is repeated layer after layer until the metal section is finished. Each layer was vertically deposited, perpendicular to the layer that came before it, to promote better layer formation and lessen porosity and fissures. A continuous deposition causes the layers to melt and build up heat, which causes a wide range in the size of the layers. The inter-pass cooling strategy was carried out to ensure the quality of the sample. This process is accompanied by the use of the robotic-arm which does the welding work. The parts of the wire arc additive manufacturing machine are depicted below in figure 1.2.

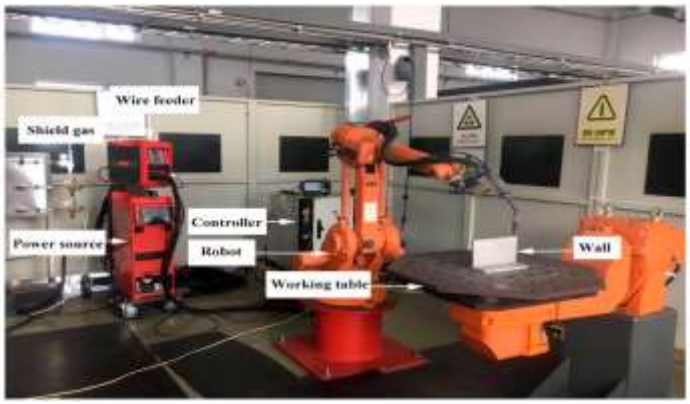

Figure 1.2 Parts of WAAM

1.2 Significance of WAAM:

The idea behind WAAM first emerged in 1926, when a scientist by the name of Baker obtained a patent for using an electric arc as a heat source to create three-dimensional things. Shape welding was utilised to create massive, high-quality nuclear steel components in 1983. Large-scale metal part manufacturing is a specialty of WAAM. In contrast, metal additive manufacturing (AM) processes using powder bed fusion (PBF) often result in smaller, higher-definition components. In contrast to PBF AM machines, which have a constrained build envelope, a WAAM machine's robotic arm has more flexibility of movement, therefore the size of a component is only constrained by the distance that the arm can go. When compared to PBF techniques, this enables the manufacture of larger pieces. The welding wire used in the WAAM printing process is much less expensive in terms of material prices than the metal powder used in metal PBF. This is because welding, a well-established manufacturing method in and of itself, forms the foundation of WAAM technology. The standard WAAM hardware consists of inexpensive welding tools that are easily available and less expensive than a number of commercially available metal 3D printers. Additionally, handling wire typically requires less particular safety equipment than handling powder, which requires it. The high density and robust mechanical characteristics of WAAM-produced parts, which are comparable to those of parts made using conventional manufacturing techniques, are particularly noteworthy. Due to the fact that the wire feedstock is a dense input material, very little porosity is introduced throughout the fabrication process, producing an extremely dense end item. Additionally, WAAM is a strong choice for activities involving the repair and maintenance of particular parts, such as turbine blades, molds, and dies. With WAAM, worn-out features or broken components can be fixed by applying fresh material to their surface. As there is no need

to create a new part from the start, this can save money in a big way.

1.3 Limitations of WAAM:

Heat management is one difficulty with WAAM. High temperatures are used throughout the printing process, which contributes to the buildup of residual stress, a problem frequently encountered with metal 3D printing. Cooling must be considered since residual stress frequently causes deformations in a component. Shielding is required to produce an inert atmosphere when employing specific materials, such as titanium, to assure the proper building conditions. This dictates that an inert gas chamber must be used for the process. However, the installation of an inert gas chamber will raise the cost of the machinery and restrict the size of items that may be produced using this method. WAAM often creates pieces with a rough surface finish that are close to net form, hence the surface of a part needs to be finished via machining.

2. WAAM of significant functional metals

2.1 HASTELLOY

Hastelloy is a alloy of nickel with molybdenum and chromium majorly with minimum amount of Iron, Tungsten, and Cobalt The alloy is used to make high-temperature gas path components for the chemical industry's pipes and valves as well as for turbine combustors, flame holders, liners, pressure vessels for some nuclear reactors, chemical reactors, and pressure vessels. It is used in oil and gas industry. Hastelloy is a corrosion-resistant nickel alloy with additional chemical components like molybdenum and chromium. This substance is resistant to corrosion and high temperatures. Numerous studies have been conducted on the Hastelloy additive manufacturing process. Much of salient observations reported in WAAM of Hastelloy is shown in Table 1.

Table 1 WAAM of Hastelloy

S.no	Material Grade	Author	Details	Input parameters	Salient Observations
1	Hastelloy C-276	Rajesh Kannan et al	Layer by layer deposition with SS904L substrate of Hastelloy with 1.2 diameter wire.	welding current- 160 Amps voltage- 16.4 V, welding speed-250 mm/min, Deposition rate 1.18 Kg/h	Tensile strength (UTS)-680.73Mpa, yield strength (YS) - 311.08 MPa, Fatigue resistance for 2 x 10^6 cycles - 156 Mpa (Minimum fatigue)
2	Hastelloy C-276	Qiu et al	Shielding gas cover 15 L/min, Interpass dwell time-60 s, Electrode to workpiece-3 mm Wire feeder and substrate-30°	Current-140A, Arc voltage- 13V Torch travel speed-100 mm/min Wire feed speed-1000 mm/min Welding torch-10 L/min	UTS and YS average values for horizontal samples (469 52 MPa and 287 50 MPa, respectively) are higher than for vertical samples (399 12 MPa and 186 27 MPa
3	Hastelloy C-22	Perez-Soriano et al	Powder material fed to the plasma jet by injected with a pressurized gas (powder gas, 1.5 L/min), argon	current 120–250 A, speed 100–400 mm/min, material feed rate 11–43.5 g/min	YT of air (332.32 MPa; 21.36 MPa) and argon (338.14 MPa; 9 MPa) without heat treatment
4	Hastelloy C-276	ZhijunQiu et al	a zig-zag deposition path, coupled with active cooling and interlayer temperature control.	Heat inputs (276, 368, and 553 J/mm)	Modified bulk texture, refined dendritic arm spacing, and reduced chemical segregation
5	Hastelloy C-276	Bintao Wu et al	coated with creep-resistant steel P91	Specimens with and without heat treatment	Precipitation and grain size, boundaries, orientation, and hardness distribution. The ratio of high-angle grain boundaries (HAGBs).

Rajesh Kannan et al [1] observed the functionally graded SS904L material produced using wire arc additive manufacturing and the microstructural characteristics of Hastelloy C-276. The components now have an enhanced tensile strength of 680.73 MPa and yield strength of 311.08 MPa owing to the wire arc additive

manufacturing process. Additionally, it demonstrated 156 Mpa of fatigue resistance after enduring 2 x 106 cycles. This is as a result of the altered microstructure, which now has more equiaxed and columnar dendrites as well as observable inhomogeneous characteristics along the constructed direction. Compared to SS904L wrought counterparts, the fatigue strength was 28–35% lower.

Qiu et al [2] observed the mechanical and microstructural characteristics of wire arc additively manufactured Hastelloy C-276. In this study, a wall is constructed, and various orientations were used to examine the mechanical qualities. The findings demonstrate that the emergence of anisotropy and heterogeneity in the observed mechanical characteristics is caused by changes in the primary dendrite arm spacing, dislocation density, and second-phase precipitates along the path of the material's deposition. The consistent dendritic formations boost the toughness. The tensile test sample is developed to evaluate the microstructure and different mechanical properties. Hastelloy C276 GT-WAAMed has an intermetallic p phase-scattered interdendritic region and a Ni- matrix with directed elongated columnar dendrite dominance. Only the bottom sections contain Ni2Mo4C carbide, which may be because there was more time for heat to build up there than there was in the upper regions. Subgrain boundaries can be created by a vast variety of dislocations, and their frequency appears to rise from top to bottom. Anisotropy in mechanical characteristics results from changes in microstructure. The elongated dendrites in the matrix are thought to be responsible for the higher tensile strength but lower ductility of the horizontal samples (x-y plane) compared to the vertical samples (y-z plane). Strong directed dendrites that predominate with microstructural evolution can be used to explain why the microhardness of the as-deposited specimens is evenly distributed over different regions. UTS and YS average values for horizontal samples (469 52 MPa and 287 50 MPa, respectively) are higher than for vertical samples (399 12 MPa and 186 27 MPa). Both directions have great ductility qualities, although their values differ. The x-y plane has a decrease in elongation of 43 6%, whereas the y-z plane has a greater increase in ductility of 55 ± 3%. It also exhibited various fracture behavior.

Perez-Soriano [3] This study's goal was to ascertain how two distinct heat treatments and the atmosphere processing conditions (air and argon) affected the characteristics of specimens made from the nickel-based alloy Hastelloy C-22 by plasma transferred arc (PTA). The parameters for additive manufacturing were first optimised. Then, two walls of air and argon were built. Then a predetermined number of specimens were cut out and evaluated. Three specimens from each wall were examined as-built samples for comparison with the extracted specimens from both walls. Moreover, a heat treatment that is frequently employed. For further comparisons, a typical Hastelloy heat treatment with two distinct cooling techniques was chosen. After the heat treatment, three of them were cooled down using rapid air cooling (RAC), while the other three were cooled down using water quenching (WQ). To find out how much the processing circumstances affected the final characteristics of the created specimens and how thermal treatments could alter them, a thorough characterization was carried out. Phases were found and precipitates appeared as the heat treatment was altered, according to X-ray diffraction and microstructural analyses. Additionally, the outcomes of testing mechanical and tribological parameters revealed slight variances brought on by changes in the processing environment. The yield strength of the two detached specimens from the walls attained values closer to the norms in air (332.32 MPa; 21.36 MPa) and argon (338.14 MPa; 9 MPa) without heat treatment. However, the effect of the cooling rate was less helpful than expected, lowering the deformation properties of the specimens below 11%

regardless of the production atmosphere (air or argon) or the cooling rate technique.

ZhijunQiu [4] , A Ni-based Hastelloy C276 alloy was created in this study employing cold metal transfer (CMT)-based directed energy deposition (DED) with a zig-zag deposition path, coupled with active cooling and interlayer temperature control. Through effective interlayer temperature control, analogous mechanical characteristics were attained for the produced alloys under varied heat inputs (276, 368, and 553 J/mm). DED's large-scale industrial fabrication and deployment of Hastelloy C276 is facilitated by such a broad processing window. Despite this, lower heat input appears to marginally refine the microstructure and lessen the mechanical anisotropy of produced alloys, which is attributed to the combined effects of modified bulk texture, refined dendritic arm spacing, and reduced chemical segregation under lower heat input. Despite variations in geometrically necessary dislocation (GND) densities with heat inputs, no significant change in the average total dislocation density (TDD) in the microstructure of all samples was observed as suggested by the peak profile analysis of Synchrotron X-ray diffraction data, which is beneficial for lowering solidification cracking susceptibility. Furthermore, all of the as-fabricated alloys have a typical strong fiber-type (200) crystallographic bulk texture as assessed by neutron diffraction, but this texture was substantially weaker in the lowest heat input condition. This work introduces a unique approach for stable additive manufacture of Hastelloy C276 alloy, as well as rationales for stabilized attributes based on insights into microstructure and bulk texture developments achieved through multiple techniques.

Bintao Wu [5] In this study, a new structure for nuclear purposes was designed using nickel-based Hastelloy C276 alloy coating on creep-resistant steel P91. Using a variety of microscopy techniques and hardness testing, the microstructure of cladding systems with/without post-heat treatment was investigated, including precipitation and grain size, boundaries, orientation, and hardness distribution. The results demonstrate that the as-cladded structure has extremely hierarchical variability, which is mostly due to the exceptionally coarse-grained microstructure in the heat-affected zone on the steel side and generally columnar dendrites generated on the Hastelloy side. The specimen has re-oriented grains and a homogenized microstructure after tempering heat treatment. Meanwhile, the ratio of high-angle grain boundaries (HAGBs) in steel regions increases dramatically, and hardness values become more evenly distributed. This research establishes a strong metallurgical link between two structural materials and provides insights into the production of dissimilar metal components with site specific characteristics.

2.2 INCONEL

Inconel alloys are oxidation-corrosion-resistant substances that are ideal for use in harsh conditions susceptible to pressure and heat. Inconel generates a thick, persistent, passivating oxide layer during heating that shields the surface from additional damage. Inconel is appealing for high-temperature applications because it maintains strength over a wide temperature range, unlike steel and aluminium, which would creep due to thermally-induced crystal voids. Depending on the alloy, precipitation hardening or solid solution strengthening is used to develop the high-temperature strength of inconel.Extreme environments are where Inconel frequently appears. It is frequently found in turbocharger rotors and seals, electric submersible well pump motor shafts, high temperature fasteners, chemical processing and pressure vessels, heat exchanger tubing, steam generators, and core components in nuclear pressurized water reactors. It is also frequently found in gas turbine blades, seals, and combustors. The salient observations noted in WAAM of Inconel is shown in Table 2.

Table 2 WAAM of Inconel

S.No	Material Grade	Author	Details	Input Parameters	Salient Observations
1	Inconel 625	Mohammed Tanvir	Melted and deposited additively through a cold metal transfer (CMT)-based WAAM process. The deposited specimens were heat-treated at 980 °C for 30, 60, and 120 min	Heat-treated at 980 °C for 30, 60, and 120 min	The orientation and size of the columnar dendrites remain almost the same throughout the microstructures. Heat treatment localized the Nb content of the sample with small irregular shapes, which are mainly MC-type carbides.
2	Inconel 625	Owais Mansoor	Deposited with good forming quality by using a layer-by-layer deposition strategy. Different microstructures were identified at the different layers of the specimen, with the bottom layers consisting mainly of fine primary cellular structures	Current 120–250 A, Speed 100–400 mm/min Temperature - 500 °C -2000 °C	The precipitate formation was observed as the samples were heated to a temperature beyond 1000℃.
3	Inconel 625	Safarzade	Under as-prepared and heat-treated circumstances, the microstructure and mechanical characteristics of Inconel 625 alloy manufactured by wire arc additive manufacturing were examined.	Aging heat treatment M23C6 carbide	Solution heat treatment increased hardness and yield strength while decreasing elongation, but it had no effect on tensile strength.
4	Inconel 625 and 308L SS	Tianzu	Dual-wire arc additive manufacturing was employed in this study to create a functionally graded material (FGM) with a seamless composition transition from 100% Inconel 625 (IN625) to 100% stainless steel 308 L, with the composition transition occurring along the torch-traveling direction.	Composition transition occurring along the torch-traveling direction. Low-melting-temperature-eutectic phase	Reducing the heat input per unit height increases tensile strength and elongation by 39.5% and 221.7%, respectively.

Mohammed Tanvir Inconel 625 [6], is melted and deposited additively through a cold metal transfer (CMT)-based WAAM process. The deposited specimens were heat-treated at 980 °C for 30, 60, and 120 min and then water quenched to investigate the effect of heat treatment on microstructure and phase transformation and to identify the optimum heat treatment condition. The microstructure of the Inconel 625 is composed mainly of columnar dendrites. The morphology of the microstructure does not change significantly due to heat treatment for different time periods at 980°C. The orientation and size of the columnar dendrites remain almost the same throughout the microstructures. The as-deposited sample contains brittle leaves phases, which are not found in the heat-treated samples. Heat treatment localized the **Nb** content of the sample with small irregular shapes, which are mainly MC-type carbides. The crystal structure of the additively manufactured Inconel 625 sample mainly consists of the Ni Cr-based γ-phase. Unwanted delta phases are formed due to heat treatment, then the expected time, which is due to the localization of Nb content at the interdendritic spaces. The size of the MC carbide and the presence of the delta phase percentage increase with increasing heat treatment time. The microstructure is pore-free in both the as-deposited and heat-treated conditions.

Owais Mansoor Inconel 625 [7] was deposited with good forming quality by using a layer-by-layer deposition strategy. Different microstructures were identified at the different layers of the specimen, with the bottom layers consisting mainly of fine primary cellular structures. As the distance from the interface increased, the main structure became columnar dendrite with classical secondary dendrite arms, and the sample microstructure of the last layer tends to form an equiaxed structure. As the temperature was increased, the cellular branching of the dendrites in the microstructure reduced leaving behind small independent strands until finally the complete disintegration of the dendritic structure was observed at 1200℃. With the

increase in temperature for heat treatment, the hardness at a point first increase than is found to decrease slightly as the temperature reaches 1200℃. This is due to the complete disintegration of the dendritic structure at such very high temperatures. And it is observed that the UTS and % elongation of the sample is maximum at the bottom layer and decreases gradually on moving upwards. The precipitate formation was observed as the samples were heated to a temperature beyond 1000℃. This was due to the presence of a small % of Molybdenum in the composition which reacts with the atmospheric oxygen to form metal oxide.

Safarzade [8], Under as-prepared and heat-treated circumstances, the microstructure and mechanical characteristics of Inconel 625 alloy manufactured by wire arc additive manufacturing were examined. The microstructure of the as-prepared alloy formed a dendritic Ni-based solid solution phase, as well as (Nb, Ti)C carbide, Laves, and -Ni3Nb secondary phases. The dissolution of the Laves and Ni3Nb phases was caused by solution heat treatment. Dendrites were also replaced by massive columnar grains. Aging heat treatment produced grain boundary M23C6 carbide and nanometric" precipitates. The as-prepared part's hardness, yield, and tensile strengths, as well as elongation, were comparable to those of the cast alloy, and fracture occurred in a transgranular ductile mode. Solution heat treatment increased hardness and yield strength while decreasing elongation, but it had no effect on tensile strength. Furthermore, aging heat treatment deteriorated the tensile characteristics and transformed the fracture mode to a mixture of transgranular ductile and intergranular brittle.

Tianxu [9] Dual-wire arc additive manufacturing was employed in this study to create a functionally graded material (FGM) with a seamless composition transition from 100% Inconel 625 (IN625) to 100% stainless steel 308 L, with the composition transition occurring along the torch-traveling direction. With such a composition transition, the place with the worst mechanical qualities in the composition gradient path might be clearly and easily recognized, allowing the issue to be completely exposed. Cracks were discovered near the position with IN625 of 20% wt during manufacture. They were identified as liquidation fractures, which belong to hot cracks, after examining the fracture morphology and crack location. The low-melting-temperature eutectic phase is created by the segregation and aggregation of carbides at the grain boundary, which is liquefied into the liquid film by the heating of the following layers and is subsequently driven apart by residual stress. The cracks always developed near the position with IN625 of 20% wt, where the FGM has the highest crack sensitivity, according to the experimental results and phase diagram calculations. As a result, it was determined to be the FGM's weakest place, and its weakening mechanism could be clarified more easily due to the composition transition, which presents a high probability of obtaining improved mechanical properties if a more targeted optimization strategy is used. Although process parameter optimization reduces the heat input per unit height to thin dendrites and alleviates cracking, cracking still occurs in the weak composition range. By removing the corresponding composition range, the composition gradient route optimization can more comprehensively solve the cracking issue, and the tensile strength and elongation increased by 39.5% and 221.7%, respectively, considerably improving the mechanical properties of the FGM. Secondary phases, such as MC and Laves, gather at grain boundaries due to the segregation of solid solution strengthening elements such as Nb and Mo, resulting in weak grain boundaries and reduced solid solution strengthening, which leads to weak mechanical properties and a high crack susceptibility. The liquation cracks in the FGM invariably appear near the position with 20 wt% IN625. It is induced not only by the weakening of dislocation and precipitation strengthening, but also by an

increase in crack sensitivity caused by a change in solidification mode and composition. These criteria determine the FGM's weak locations. By removing the weak composition range, the composition gradient route optimization can more comprehensively solve the crack issue for the FGM with composition transition along TTD. When compared to process parameter optimization, reducing the heat input per unit height increases tensile strength and elongation by 39.5% and 221.7%, respectively, after composition gradient path optimization.

Alonso [10], In this study the final geometry and post-processing machining step is concentrated. Inconel 718 walls were fabricated in a controlled environment and their microstructure and mechanical properties were studied in this study. Following that, slot milling operations were carried out to study the effect of cutting speed and machining direction. The insights collected from this article can be utilized as a guide for defining strategies and milling parameters correctly. It was discovered that greater cutting speeds result in improved surface quality and reduced torques. it demonstrates the effect of WAAMInconel 718 anisotropy on its machinability. Milling in the torch travel direction provides greater dimensional accuracy values with lower cutting torques than machining in the building direction. During the WAAM production process, a fine dendritic microstructure was formed. As a result of the directional heat flow, a columnar grain distribution was found in the construction plane (YZ), but it was largely equiaxial at the outer surface in the deposition plane (XZ). Lave phases and carbides were also discovered in the interdendritic area due to nonequilibrium cooling circumstances. The mechanical properties of the WAAM alloy outperformed those of the as-cast alloy. The yield and tensile strengths, however, were greater in the travel direction (X axis) than in the construction direction (Z axis). This mechanical anisotropy could explain why cutting torque and bending moments are lower when machining in the building direction. As the cutting speed increased, so did the machining forces. This impact can be explained by the reduction in plastic deformation caused by greater temperatures during chip removal. Milling flaws such as top burrs were also discovered and were more visible at higher cutting speeds. Furthermore, independent of the machining direction, the surface roughness improved with increasing cutting speed. Within the investigated cutting parameters, milling with the highest cutting speed (60 m/min) in the building direction produced the best average surface roughness (Ra= 0.258 m). With increased cutting speed, narrower grooves were obtained. This outcome could be attributed to the tool's decreased bending moment in the direction perpendicular to its forward motion.

Benakis [11], Gas Tungsten Arc Welding, the effects of high and low frequency pulsed currents on the weld geometry and heat affected zone are investigated (GTAW). The materials used in this experiment were Ti-6-4 and Inconel 718, both of which are widely used in aerospace applications due to their high strength-to-weight ratio and high-temperature strength, respectively. The test was developed using a Taguchi-inspired orthogonal array to vary the torch travel speed controlled by an industrial robotic arm and to change the wire feed speed in addition to the current mode and value. The results show that the dual pulse combination of high and low frequency pulses can handle both weld size and penetration depth and heat affected zone. Changing from wide, deep-penetration beads to high-aspect-ratio, narrower beads has been proven in a single manufacturing setup, allowing the WAAM process to evolve. Table 3.5 shows the welding input parameters for his IN718 wire on the SS316L panel.Weld bead parameters such as reinforcement cap height and bead width, and penetration depth can be adjusted using a combination of high and low frequency pulses, as well as changes in travel speed and wire feed rate. The lower heat input and arc confinement induced by radio

frequency pulses can also be used to reduce the heat affected area by reducing the root base of the heat affected zone. With the same experimental setup available for WAAM, the technique studied allowed the production of both high-penetration/wide bead welds suitable for the root pass and low-penetration/narrow bead welds excellent for the root pass. A secondary location is suitable. This approach yielded comparable results in his Inconel-718 and Ti-6-4 commissioning using a Taguchi-inspired orthogonal array design. Future research is needed to optimize the output of each current mode for specific applications and to validate the impact of the process on additive manufacturing

2.3 ALUMINUM

Aluminum has a density that is around one third that of steel, which is lower than that of most common metals. It has a strong affinity for oxygen, and when exposed to air, creates a protective oxide coating on the surface. Aluminum visually resembles silver due to similarities in colour and light-reflecting properties. It is ductile, soft, and non-magnetic. Aluminum is the twelfth most prevalent element in the universe based on the frequency of its one stable isotope, 27Al, which is also the only stable isotope. Radiodating makes use of 26Al's radioactivity. Most often, aluminum is alloyed, which significantly enhances its mechanical qualities, especially when it is tempered. For instance, typical aluminum foils and beverage cans are made of alloys that range from 92% to 99% aluminum. [144] Copper, zinc, magnesium, manganese, and silicon (such as duralumin) are the primary alloying elements, with small amounts of other metals (a few percent by weight) present. The salient observations of WAAM in Aluminum is listed in Table 3.

Table 3. WAAM of Aluminum

S.No	Material Grade	Author	Details	Input Parameters	Salient Observations
1.	ER2319 and ER5087 (2024 AL)	Zewu Qia, Bojin Qi	Double Wire + Arc Additive Manufacturing and A heat treatment process (solution + natural/artificial aging)	current: +100A/-120A, frequency:100 Hz feed speed-1.5 m/min and 2.4 m/min travel-speed (300 mm/min), arc length (5 mm), flow rate of 99.99% argon shielding gas (15 L/min)	Heat treatment can significantly affect the microstructure and mechanical properties of WAAM 2024 alloy
2.	2219 Al	Yinghui Zhou	Relationship between copper distribution and strength in WAAMed 2219 Al alloy	Solution temperature at 540 °C, 530 °C, and 520 °C, respectively.	The average ultimate tensile strength, yield strength, elongation, and micro-hardness of the WAAM processed samples were obtained after T6 treatment with 540 °C, 45 min/Water quenching +180 °C, 6 h/Water quenching, which is 397 ± 4 MPa, 303 ± 5 MPa, 5.3 ± 1%, and 139 ± 6 HV respectively.
3.	2319 Al	Xuewei Fang and Lijuan Zhang	The peening process can improve the mechanical properties of WAAM-treated 2319 aluminum alloy.	Peening process and hammering the microstructure of the samples	Mechanical properties are greatly improved by hammering at 50.8% deformation. Yield strength and tensile strength increased by 60.6% and 13%, respectively.
4.	5A06-Al Alloy	Haibin Geng, Jinglong Li	Aim to reveal the geometrical constraints and mechanical property indices using experimental methods. Among the deposition parameters in the paper, angles greater than 20 are preferred for WAAM.	Travel speed, m/min - 0.25, Peak current, A-160, Wire feed speed, m/min-2.0, Layer height, mm-1.3	The average values of tensile strength, yield point and elongation are 273 MPa, 124 MPa and 34% respectively.
5.	AA5183	A. Horgara, H. Fostervoll	Deals with wire arc additive manufacturing of AA5183 aluminum alloy using conventional gas metal arc welding deposits on 20 mm thick AA6082-T6 plates as support material. increase	The wire was 1.2 mm diameter solid wire of AA5183, which is an Al4.5MgMn alloy	Tensile testing gave mean values of yield and tensile strength of 145 and 293 MPa, respectively. Hardness measurements gave HV1 of around 75 kg/mm2 in the horizontal direction, while 70–

					75 kg/mm2 was found in the vertical direction
6..	Al	Tawfik	Deposition parameters should be adjusted in real time during the WAAM process using artificial intelligence (AI) methods. Reducing the heat input increases the solidification rate and reduces the volume fraction and size of the equiaxed grains.	WFS 2 m/min TS 150, 250, 350, 450 mm/min Current-150 A, AC	The UTS and YS increased by 11.58 % and 11.96% respectively. Elongation increased by 45.45 % when TS increased from 150 to 450 mm/min.
7.	AA-5183	Lavinia Tonelli	The morphological, mechanical, and microstructural features of aluminum sheets fabricated by wire and arc additive manufacturing (WAAM) using ER5183 wire were evaluated.	Current-30–50 A Welding Speed-12–15 mm/s, Wire feed rate-2–3 m/min Layer height-0.5–2 mm	Chemical composition of WAAM plates complied with the standards for AA 5183.The deposition process resulted in a layered structure comprised of successive solidified melt pools and the final microstructure of WAAM plates was composed by α-Al phase and fine Fe- and Mg-based intermetallic particles homogeneously distributed in the aluminum matrix.
8.	5356 Al alloy	Jiankun Wang	5356 aluminum alloy CWW was used for WAAM to analyze the macromorphology, microstructure and mechanical properties of the thin-walled alloy.	Shield gas type-100% Ar,Shield gas flow rate-10–20 L/min,Arc voltage-14–15 V	Heat accumulation and slow heat dissipation at the top and middle of the sample lead to grain coarsening, while heat dissipation at the bottom through the substrate is faster, resulting in smaller grains.
9..	AA2196 Al-Li alloy	Chengpeng Xue	The effects of hot working and T6 post-deposition heat treatment on the micro porous defects and mechanical properties of AA2196 Al-Li alloy.	Hot working and T6 post-deposition heat treatment on the micro porous defects. Faster cooling rate during the WAAM process	XCT has been used to quantify chains of micro porosity flaws in WAAM Al-Li alloys. By using 42% hot deformation, mechanical characteristics of WAAM Al-Li parts can be greatly enhanced. At the regions of 1/4-1/2 thickness, the compression stress has a significant impact on how well micro pores close.
10..	2219 Al alloy	Yinghui Zhou	Several arc TS values, he used WAAM to successfully produce 2219 thin-walled aluminum alloy parts.	Maximum values when TS is 350 and 250 mm/min,	TS of 350 mm/min possessed finer equiaxed grain and exhibited higher ultimate TS (273.5 MPa) and yield strength (182.9 MPa) compared to those fabricated at 250 mm/min.

Zewu Qia, Bojin Qi [12] found that 2024 aluminum alloy cannot be produced by conventional single wire + arc additive manufacturing technology. By feeding two wires (ER2319 and ER5087) at the same time and adjusting the wire feeding speed, the deposition of 2024 aluminum alloy can be achieved by the double wire + arc additive manufacturing method. A heat treatment process (solution + natural/artificial aging) was performed to further improve the properties. As-deposited and heat-treated he tested and analyzed the microstructure and mechanical properties of 2024 aluminum alloy deposits. The microstructure of the as-deposited WAAM 2024 alloy was mainly composed of equiaxed (non)dendritic and columnar dendrites in the inner layer region and equiaxed (non)dendritic in the intermediate layer region. The tensile properties of the as-deposited WAAM 2024 alloy exhibited isotropic and anisotropic properties after heat treatment. Heat treatment increases strength and elongation in the transverse direction, but reduces elongation in the machine direction. Heat treatment can significantly affect the microstructure and mechanical properties of WAAM 2024 alloy. Elimination of porosity and reduction of property anisotropy should also be pursued for further research and applications.

Yinghui Zhou [13] observed that a relationship between copper distribution and strength in WAAMed 2219 Al alloy was established. Then the effects of solution

conditions on their microstructure and mechanical performance were analyzed. Some conclusions can be drawn as follows. The precipitation strengthening of the θ" phase in the aged aluminum alloy WAAMed 2219 is affected by the solution temperature. As the temperature of the solution is increased from 520 to 540 ºC, the highly supersaturated sample can contain a large amount of uniformly distributed θ phase at the nanoscale. 540ºC is a suitable melting temperature for aluminum alloy WAAMed 2219. For the amounts of dissolved copper in the WAAMed 2219 aluminum matrix of 6.95, 7.07, and 7.64%, the YS increments (180 °C × 6 h/WQ) of the θ″ phase after aging are 150.3, 165.2, and 202.1 respectively MPa.

Xuewei Fang and Lijuan Zhang [14] observed that the peening process can improve the mechanical properties of WAAM-treated 2319 aluminum alloy. The following conclusions can be drawn: Hammer The microstructure of the samples struck with is composed of fine-grained and coarse-grained regions, where the width of the coarse-grained region decreases with increasing interlaminar strain, fine and elongated (partial) grains were produced after 50.8% strain. Mechanical properties are greatly improved by hammering at 50.8% deformation. Yield strength and tensile strength increased by 60.6% and 13%, respectively. However, the elongation of the as-peened samples decreased significantly compared to the as-deposited samples. It turns out that the main strengthening mechanism in the peened samples is mainly due to the high density of dislocations generated by plastic deformation, with very little contribution from grain refinement and other mechanisms. Grain refinement by inter-layer peening is primarily due to recovery and static recrystallization when a new layer is deposited on top of the peened layer and the previously peened layer is subjected to in-situ heat treatment. caused by The subsequent peening process deforms the recrystallized grains again, creating dislocations within the grains.

Haibin Geng, Jinglong Li [15] WAAM is only used as a molding method to facilitate the formation of complex structures. In order to make the most of complex structural formation, it is necessary to design more optimal and more complex structures. In short, WAAM geometry optimization is gradually becoming a new research area. However, the boundary conditions for WAAM geometry optimization are unknown for most materials. In this paper, for example, we deal with wire-arc additive manufacturing aluminum alloy 5A06 and aim to reveal the geometrical constraints and mechanical property indices using experimental methods. Among the deposition parameters in the paper, angles greater than 20 are preferred for WAAM. If the angle is less than 20, the start and end sides of the angle overlap. The minimum radius of curvature that can be produced with WAAM is 10 mm with a slice width of 7.2 mm. If the radius of curvature is set smaller than this value, the inner contour will be distorted, which will interfere with subsequent deposition. In the x (horizontal) and y (vertical) directions, the tensile test results show isotropy. The average values of tensile strength, yield point and elongation are 273 MPa, 124 MPa and 34% respectively. The tensile properties are anisotropic in directions parallel and perpendicular to the direction of the texture. The average tensile strength and yield point of the samples in the direction perpendicular to the texture orientation are 251 MPa and 101 MPa. The average tensile strength and yield strength of the samples in the direction parallel to the texture orientation are 239 MPa and 90 MPa. The average elongations parallel and perpendicular to the direction of the texture are 37% and 34%.

A. Horgara, H. Fostervoll [16] This study deals with wire arc additive manufacturing of AA5183 aluminum alloy using conventional gas metal arc welding deposits on 20 mm thick AA6082-T6 plates as support material. increase. Microscopy shows that the process is workable but could be further optimized to reduce gas porosity and hot cracking.

Hardness measurements confirmed relatively high hardness. H. About 75 kg/mm² on horizontal plane, 70-75 kg/mm² on vertical plane, up to 100 kg/mm² up to AA6082 core board. Mechanical tests revealed a yield point and tensile strength of 145 MPa and 293 MPa, respectively, with the lowest values in the thickness direction (Z). Ductility was high in the parallel (X) and perpendicular (Y) directions to the film deposition direction.

Tawfik [17], WAAM is a critical manufacturing process widely adopted for industrial applications such as aircraft and aerospace parts. It is well documented that such improved properties and eliminated defects can be provided using appropriate manufacturing parameters and post-treatment of the deposited components. For future work, the following prospects and conclusions are summarized according to the above literature. Improper selection of parameters, poor programming strategies, and unstable weld pools are the main reasons for errors in WAAM for aluminum alloys. Besides, there are still some defects such as non-identical material properties, extensive defects in the deposited parts, and lack of structural uniformity. A modified GMAW process, CMT, is concluded to be the preferred manufacturing process for aluminum WAAM. Low heat input and post-treatments such as interlayer rolling and heat treatment eliminated residual stress, deformation, and pore distribution number. The applied post-treatment process plays a major role in WAAM eliminating the challenges of aluminum alloy production. However, process parameter optimization is still a complex process due to the large number of parameters that need to be optimized. Therefore, deposition parameters should be adjusted in real time during the WAAM process using artificial intelligence (AI) methods. Reducing the heat input increases the solidification rate and reduces the volume fraction and size of the equiaxed grains.The hardness test average is 73.85 HV. Hardness is highest at the bottom, second highest for him in the middle, and lowest at the top. In tensile testing, the properties of the upper and middle tensile specimens are similar. The tear strength and yield strength of the lower part are better than the rest, but the toughness is worse. Due to interlayer defects, the properties of the samples in the vertical direction are much worse than those in the lateral direction. This experiment proves that heat input affects the microstructure and mechanical properties of aluminum alloys. Therefore, properly controlling the cooling rate of aluminum alloys in AM can yield parts with different properties and bring researchers new ideas for reinforcement.

Lavinia Tonelli [18] In the current work, the morphological, mechanical, and microstructural features of aluminum sheets fabricated by wire and arc additive manufacturing (WAAM) using ER5183 wire were evaluated. For the purpose of comprehensive characterization of WAAM plates, all analyzes were performed on samples extracted along parallel (L), diagonal (D) and perpendicular (T) directions to the sedimentary layers. rice field. Based on the experimental results, we can draw the following conclusions: The chemical composition of WAAM plates meets the standard of AA5183. The deposition process resulted in a layered structure consisting of continuous solidified melt pools, and the final microstructure of the WAAM plates consisted of α-Al phases and fine Fe- and Mg-based intermetallics uniformly distributed in the aluminum matrix. made up of particles. Microstructural discontinuities (gas porosity and microcracks) were detected by microstructural analysis, especially located in the interlayer region of all samples. Consistent porosity is also demonstrated on all fracture surfaces, which is the main cause of the tensile behavior of WAAM specimens. Tensile test results showed anisotropic behavior according to the L, D and T orientations. The L direction exhibited the best tensile properties over conventional AA5083-O films. Values similar to those of the conventional alloy were recorded in the

D direction. On the other hand, the T direction was characterized by the lowest mechanical properties.

Jiankun Wang[19] In this study, 5356 aluminum alloy CWW was used for WAAM to analyze the macromorphology, microstructure and mechanical properties of the thin-walled alloy. We compared the top, middle, and bottom of the thin wall. From this study the following conclusions can be drawn: WAAM can be used with CWW to produce aluminum alloy 5356. The properties of thin metal walls are superior to those of cast aluminum-magnesium alloys. Heat accumulation and slow heat dissipation at the top and middle of the sample lead to grain coarsening, while heat dissipation at the bottom through the substrate is faster, resulting in smaller grains.

Chengpeng Xue[20] This study investigated the effects of hot working and T6 post-deposition heat treatment on the microporous defects and mechanical properties of AA2196 Al-Li alloy. The following conclusions can be drawn: Due to the faster cooling rate during the WAAM process compared to conventional casting production methods, the grain size of the WAAM alloy is 100 μm instead of over 100 μm in conventional casting. less than μm. A peak aging heat treatment can be used to obtain nano-sized T1 precipitates ranging from 90 nm to 160 nm. In addition, there is also a minor θ' amplification phase and an Ag-rich Ω amplification phase. Due to the high hydrogen supersaturation, the WAAM-Al-Li parts also exhibit considerable microporosity, with sizes reaching 10–30 μm, and some can reach 100 μm. These microporosities line the melting path and are observed to be much denser and larger in size in the intermediate sedimentary layers than in the main regions. In the absence of hot deformation, the subsequent T6 heat treatment might actually amplify this situation rather than reduce the mechanical properties by increasing the pore size. It was found that a hot deformation of 42% and a T6 heat treatment effectively closed the porosity, reducing most of it to less than 30 μm, effectively eliminating crack initiation sites. Using X-ray computed tomography (XCT) characterization and finite element method (FEM) simulations, we discovered the microporous closure mechanism. It is careful control of compressive and tensile stresses that can minimize porosity. If these two stresses are not well controlled, as in the case of the 23% reduction, microporous growth is promoted instead of microporous closure. Therefore, we successfully achieved the best performance with 42% hot working followed by T6 heat treatment, achieving a UTS of 439 MPa and an elongation of 6.9%, well over 260 MPa without hot working, A poorly hot worked elongation of 0.9 was achieved. %.

Yinghui Zhou [21] In this study, at several arc TS values, he used WAAM to successfully produce 2219 thin-walled aluminum alloy parts.The following conclusions can be drawn: When the arc TS was set at 350 and 450 mm/min, the samples showed low roughness and good forming quality. The particles became finer with increasing TS. This may be attributed to the increased solidification rate and decreased heat input. The microstructural characteristics of the layers of WAAM-treated 2219 aluminum alloy were observed. Coarse columnar and equiaxed grains were observed in the inner and interlamellar zones. Moreover, both the size and volume fraction of equiaxed grains decreased with increasing TS. The higher the TS value, the more θ phase precipitates. In the WAAM-treated 2219 aluminum alloy, the precipitation strengthening effect of the θ″ phase within grains was highest at TS 350 mm/min, and the volume fraction of θ′ phase was highest at TS 250 mm/min. The UTS and YS values of the WAAM-treated samples increased from 216.7 to 273.5 MPa and from 143.8 to 182.9 MPa, respectively, as TS increased from 150 to 350 mm/min.When TS continued to increase to 450 mm/min, , UTS dropped to 259.6 MPa, but EL increased from 450 mm/min. Both the strength and hardness of the samples were higher than

those of many other alloys reported in the literature.

2.4 STAINLESS STEEL

Steel has been a dominant material in the automotive industry for many years. Steel has also proven to be inexpensive, durable and with variable strength levels while meeting increasingly stringent engineering requirements. Steel is also very adaptable for corrective finishing work. In addition, the material has great versatility in terms of formability and the industry has reacted quickly to recognize changes due to regulatory and environmental requirements. Other advantages of steel for use in the automotive sector include ease of formability, consistency of delivery, corrosion resistance due to zinc coating, ease of joining, recyclability and excellent absorption of impact energy. (Reference - Mayank Kumar Singh, Website: www.ijetae.com (ISSN 2250-2459, ISO 9001:2008 Accredited Journal, Volume 6, Issue 7, July 2016). Used in conjunction with WAAM A low cost component can be made by using additive manufacturing compared to other additive manufacturing methods and forging standards.The main conclusions from this study are: 304L manufactured by WAAM The microstructure of stainless steel parts is filled with numerous dendrites and the direction of growth is along the temperature gradient. WAAM of stainless steel is shown in Table 4.

Table 4 WAAM of stainless steel

S.No	Material Grade	Author	Details	Input Parameters	Salient Observations
1.	SS - 308L	Van ThoaLe Dinh SiMa	Gas Metal Arc Additive Manufacturing	Thin-walled sample with dimensions of 20 mm in height and 100 mm in length.	The average vertical tensile strength (UTS), yield strength (YS), and elongation (EL) of GMAW-AM thin wall 308L are 531.78 ± 4.52 MPa, 343.67 ± 7.53 MPa, and 39.58 ± 1.38%, significantly lower than horizontal (UTS: 552.95 ± 4.96 MPa, YS: 352.69 ± 8.12 MPa, EL: 54.13 ± 1.29%).
2.	Super Duplex Stainless Steel	A.Rajesh Kanna N.Siva Shanmugam	Wire Arc Additive Manufacturing	Shielding gas of 99.9% pure argon with a constant flow rate of 20 l/min was used to deposit feeding material, ER2594 (ϕ1.2 mm) and its nominal composition (wt%) is C-0.02, Mn-0.8, W-0.01, Si-0.3, Cr-24.6, Ni-8.6, Mo-3.8, N-0.25, Cu-0.01 and Fe-balance.	The corrosion rate ranged between 1.54 and 1.61 mpy and pitting resistance was excellent compared to wrought alloy with stable micro-level pits.The PREN was > 40 and this is attributed to the increased wt% of Cr and Mo in the
3.	SHER-120G	Guang Yang	WAAM - Cold Metal Transfer	Wire feed speed - 7.0 m/min. Sheet travel speed - 16 mm/s; swing amplitude - 15 mm; scan pitch - 2.8 mm.	The ultimate tensile strength, elongation and impact toughness reach 1221 MPa, 11.76% and 63 J, respectively.
4.	SS - 321	Xiaoli Wang	WAAM-CMT	The preheating temperature was 30–50 °C,nterlayer temperature was ≤100 °C,inter-channel offset was 3–3.5 mm,shielding gas was a 90% Ar and 10% He premix at a gas flow of 15–20 L·min−1.	There were a white austenite matrix and black ferrite, and a small amount of skeleton and worm ferrite was distributed on the white austenite matrix. The average hardness value from the top to the bottom region was approximately uniform, indicating that the SS 321 workpiece had good consistency. The corrosion properties of the SS 321 workpiece and the SS 321 sheet were studied in 0.5 mol/L H2SO4 solutions.

Van ThaoLe Dinh SiMa [22] In this article, gas metal arc welding (GMAW-AM) based additive manufacturing was used to produce thin walled parts from 308L stainless steel. The microstructure and mechanical properties of the constructed thin walls were investigated. The results show that the GMAW-AM thin-walled 308L is mainly composed of columnar dendrites growing along the buildup direction as the number of sedimentary layers increases. The microstructure of GMAW-AM thin-walled 308L is mainly composed of two phases. A small amount of the δ-ferrite phase that

appears within the γ-austenite dendrites. The microhardness of building materials ranges from 155 ± 1.20 HV0.1 to 169 ± 5.67 HV0.1. The average vertical tensile strength (UTS), yield strength (YS), and elongation (EL) of GMAW-AM thin wall 308L are 531.78 ± 4.52 MPa, 343.67 ± 7.53 MPa, and 39.58 ± 1.38%, significantly lower than horizontal (UTS: 552.95 ± 4.96 MPa, YS: 352.69 ± 8.12 MPa, EL: 54.13 ± 1.29%).

A.Rajesh Kannan N.Siva Shanmugam [23] Super Duplex Stainless Steel (SDSS), due to its excellent corrosion performance and strength, is widely used in highly corrosive industries such as oil and gas, petrochemical, pressure vessel and seawater equipment industries. Primarily designed for the environment. Wrought SDSS alloys are more costly to manufacture compared to austenitic stainless steels, so other techniques should be explored to produce SDSS structural components with better mechanical and corrosion properties. WAAM is a rapid manufacturing technique based on the deposition of metals in a layer-by-layer technique with improved material utilization. The wall dimensions were 130 x 120 7 mm before machining and 120 x 114 4.2 mm after machining. The microstructures of different regions of the WAAM-treated SDSS walls were recorded using metallurgical microscopy and scanning electron microscopy (SEM).

GuangYang [24] Cu precipitation strengthening in maraging steels has received considerable research attention and has become the gold standard for the development of high-strength low-carbon steels. Chemical composition of the developed maraging steel welding wire SHER120-G. Thin-walled components were deposited on HE Q345 steel substrates with a thickness of 15 mm. The parameter settings are: Wire feed speed - 7.0 m/min. Sheet travel speed - 16 mm/s; swing amplitude - 15 mm; scan pitch - 2.8 mm. A mixture of Ar (98%) + O2 (2%) was used as coaxial protection. The arc was extinguished for 120 seconds after depositing one layer to ensure proper interlayer temperature so that the melt pool would not overflow during subsequent depositions. Single layer height is about 2.7mm. 200mm x 20mm x 120mm the two thin-walled components were manufactured by his WAAM-CMT. One of them was used for sediment analysis and the other was analyzed after direct aging.

Xiaoli Wang [25] In this study, the microstructure and corrosion properties of multi-track, multi-layer 321 stainless steel workpieces produced by a CMT-WAAM system were studied. The results showed that the microstructure of the SS 321 workpiece was regularly and periodically repeated from top to bottom from the overlap remelting zone to the interlayer remelting zone and the primary melting zone. There was a white austenitic matrix and black ferrite, with a small amount of skeleton and warm ferrite dispersed over the white austenitic matrix.

CONCLUSION

Studying materials such as Hastelloy and Inconel provides information on optimal parameters leading to better mechanical properties, as shown in Table 1-5. The study of the optimal parameters and the effect of heat on Hastelloy has not been done in detail. Future research should focus on the cracking, heat affected zone, cooling rate, magnetic field effect and heat treatment process of Hastelloy components. The mechanical properties of Inconel along the machine direction are revealed from this literature analysis. The compression temperature is determined as 950 °C. The duration of the heat treatment, the temperature of the heat treatment, and the influence of the magnetic field are analyzed. This proves that Inconel has advantages over other manufacturing processes for arc wire additive manufacturing. Various optimization techniques are used to arrive at the optimal process parameters. This can be done with Hastelloy. The materials Inconel and Hastelloy can also be analyzed in detail along with their corrosion behavior. Applications of Inconel and Hastelloy should be investigated intensively.

Moreover, WAAM technology for aluminum parts is an important manufacturing process that is expected to be widely used in industrial applications such as aircraft and aerospace parts. It is well documented that such improved properties and eliminated defects can be provided using appropriate manufacturing parameters and post-treatment of the deposited components. For future work, the following prospects and conclusions are summarized according to the above literature. Improper selection of parameters, poor programming strategies, and unstable weld pools are the main reasons for errors in his WAAM for aluminum alloys. Besides, there are still some defects such as non-identical material properties, extensive defects in the deposited parts, and lack of structural uniformity. A modified GMAW process, CMT, is concluded to be the preferred manufacturing process for aluminum WAAM. Low heat input and post-treatments such as interlayer rolling and heat treatment eliminated residual stress, deformation, and pore distribution number. The applied post-treatment process plays a major role in WAAM eliminating the challenges of aluminum alloy production. However, process parameter optimization is still a complex process as many parameters need to be optimized. Therefore, deposition parameters should be adjusted in real time during the WAAM process using artificial intelligence (AI) methods. Reducing the heat input increases the solidification rate and reduces the volume fraction and size of the equiaxed grains. Also, the mechanical properties of the WAAM-deposited components were strongly influenced by the properties of the wire material. The strength characteristics of welded parts are improved by adding elements such as powders of magnesium and titanium in appropriate amounts. A back-to-back construction strategy has been proposed as a possible process for strain relief and residual stress balancing.

WAAM stainless steel has proven to be a cost effective (compared to the PBF-AM process) and highly efficient AM process for manufacturing large-scale stainless-steel parts. His recent studies on WAAM of various stainless steels were reviewed in terms of macroscopic properties, microstructural evolution, post-heat treatment, residual stress and strain, defects, and mechanical properties. The macroscopic properties of WAAM stainless steel parts are closely related to wire feed and scan speeds, welding current mode, cooling time, and interpass temperature. Further research is needed to optimize the above process parameters to improve the dimensional accuracy and surface quality of WAAM parts. The thermal history of the WAAM process plays an important role in controlling the microstructure. B. Ratio of austenite phase to ferrite phase. Therefore, it is possible to control the microstructure by controlling the process parameters. changes in material composition, etc. B. The use of double wires is another effective approach to achieve the desired final microstructure. Subsequent heat treatments can also significantly affect and change the final microstructure. Therefore, a thorough understanding of the solidification behavior and phase transformations during the complex WAAM thermal cycle and their interrelationships with material composition, process parameters and heat treatment parameters is very important to obtain the desired microstructure in WAAM stainless steel parts. It is important. Final microstructure. Residual stress and thermal history have a significant impact on the deformation of WAAM parts. Both effects increase with increasing amounts of components. Internal stress can lead to part deformation, dimensional inaccuracy, defects, and poor mechanical properties. Phase transformations, especially martensitic phase transformations, have a large impact on residual stress reduction. Proper planning of the deposition path can also significantly reduce residual stress. Therefore, further efforts are needed to optimize the WAAM deposition path and thermal history, and to control phase transformations during WAAM to reduce residual stress and strain,

both through modeling and experimental studies.

Defects such as lack of fusion, cracks and porosity should be minimized to achieve robust mechanical properties. Precise control of heat input and heat history, proper shielding gas and tight gas seals, high quality raw materials and clean substrate surfaces help reduce defects during the stainless steel WAAM process. WAAM technology, material composition, process parameters, shielding gas composition, post heat treatment, microstructure, and defects can significantly affect the mechanical properties of WAAM stainless steels. Further understanding of the correlation between these factors and their precise control, especially the final microstructure, is important for better control of the mechanical properties of WAAM stainless steels. A major limitation of this paper is that the numerical modeling of the WAAM process is not fully explained in this paper. For future industrial applications, the fatigue properties and corrosion behavior of WAAMed stainless steels should be thoroughly studied. Moreover, further efforts are needed to improve the WAAM process to achieve faster deposition rates and better quality control.

Declaration by Authors

Acknowledgement: None

Source of Funding: None

Conflict of Interest: The authors declare no conflict of interest.

REFERENCES

1. Rajesh Kannan, A., Mohan Kumar, S., Pravin Kumar, N., Siva Shanmugam, N., Vishnu, A. S., & Palguna, Y. (2020). Process-microstructural features for tailoring fatigue strength of wire arc additive manufactured functionally graded material of SS904L and Hastelloy C-276. Materials Letters, 274, 127968. Doi: 10.1016/j.matlet.2020.127968
2. Qiu, Z., Wu, B., Zhu, H., Wang, Z., Hellier, A., Ma, Y., … Wexler, D. (2020). Microstructure and mechanical properties of wire arc additively manufactured Hastelloy C276 alloy. Materials & Design, 109007. doi: 10.1016/j.matdes.2020.109007
3. Perez-Soriano, E. M., Ariza, E., Arevalo, C., Montealegre-Melendez, I., Kitzmantel, M., & Neubauer, E. (2020). Processing by Additive Manufacturing Based on Plasma Transferred Arc of Hastelloy in Air and Argon Atmosphere. Metals, 10(2), 200. doi:10.3390/met10020200
4. Zhijun Qiu, Zhiyang Wang, Azdiar Adil Gazder, Stephen van Duin, Andrew Studer, Ulf Garbe, Qinfen Gu, Bintao Wu, Hanliang Zhu, David Wexler, Huijun Li, "Stabilised mechanical properties in Ni-based Hastelloy C276 alloy by additive manufacturing under different heat inputs incorporated with active interlayer temperature control", Materials Science and Engineering: A, Volume 862,2023,144434, ISSN 0921-5093, https://doi.org/10.1016/j.msea.2022.144434.
5. Wu, Bintao & Qiu, Zhijun & Dong, Bosheng & Muránsky, Ondrej & Zhu, Hanliang & Wang, Zhiyang & Pan, Zengxi & Li, Huijun. (2022). Microstructural characterization and hardness assessment of wire arc cladded Hastelloy C276 on creep-resistant steel P91. Journal of Materials Research and Technology. 19. 3818-3827. 10.1016/j.jmrt.2022.06.129.
6. Lei Ji, Jiping Lu, Changmeng Liua,,Microstructure and mechanical properties of 304L steel fabricated by arc additive manufacturing.https://doi.org/10.1051/matecconf/201712803006
7. Votruba, V., Diviš, I., Pilsová, L. et al. Experimental investigation of CMT discontinuous wire arc additive manufacturing of Inconel 625. Int J Adv Manuf Technol 122, 711–727 (2022). https://doi.org/10.1007/s00170-022-09878-7
8. SAFARZADE, A., SHARIFI TABAR, M., & SHAFIEE AFARANI, M. (2020). Effects of heat treatment on microstructure and mechanical properties of Inconel 625 alloy fabricated by wire arc additive manufacturing process. Transactions of Nonferrous Metals Society of China, 30(11), 3016–3030. doi:10.1016/s1003-6326(20)65439-5
9. Tianxu Li, Zhijiang Wang, Shengsun Hu, Zhenwen Yang, Ying Wang,Hot cracking during the fabrication of Inconel 625/stainless steel 308 L functionally graded material by dual-wire arc additive manufacturing,Journal of Manufacturing Processes,Volume 82,2022,Pages 461-473,ISSN 1526-6125. https://doi.org/10.1016/j.jmapro.2022.08.018.
10. Alonso, U., Veiga, F., Suárez, A., & Gil Del Val, A. (2021). Characterization of Inconel 718® superalloy fabricated by wire Arc Additive Manufacturing: effect on mechanical

properties and machinability. Journal of Materials Research and Technology, 14, 2665–2676. doi: 10.1016/j.jmrt.2021.07.132
11. Benakis, M., Costanzo, D., & Patran, A. (2020). Current mode effects on weld bead geometry and heat affected zone in pulsed wire arc additive manufacturing of Ti-6-4 and Inconel718. Journal of Manufacturing Processes, 60,61–70 Doi: 10.1016/j.jmapro.2020.10.018
12. Zewu Qi, Bojin Qi, Baoqiang Cong, Ruize Zhang Microstructure and mechanical properties of wire + arc additively manufactured Al-Mg-Si aluminum alloy DOI: https://doi.org/10.1016/j.matlet.2018.09.048
13. Yinghui Zhou, Xin Lin, Nan Kang, Weidong Huang, Zhennan Wang Mechanical properties and precipitation behavior of the heattreated wire+arc additively manufactured 2219 aluminum alloy DOI: https://doi.org/10.1016/j.matchar.2020.110735
14. Xuewei Fang a,b , Lijuan Zhang Microstructure evolution of wire-arc additively manufactured 2319 aluminum alloy with interlayer hammering.
15. Haibin Geng, Jinglong Li [14] Geometric Limitation and Tensile Properties of Wire and Arc Additive Manufacturing 5A06 Aluminum Alloy Parts. DOI: https://doi.org/10.1007/s11665-016-2480-y
16. Horgara, H. Fostervoll Additive manufacturing using WAAM with AA5183 wire DOI: https://doi.org/10.1016/j.jmatprotec.2018.04.014
17. M.M. Tawfik Enhancing the properties of aluminum alloys fabricated using wire þ arc additive manufacturing technique-A review DOI: https://doi.org/10.1016/j.jmrt.2021.04.076
18. Lavinia Tonelli Vittoria Laghi AA5083 (Al–Mg) plates produced by wire-and-arc additive manufacturing: efect of specimen orientation on microstructure and tensile properties DOI: https://doi.org/10.1007/s40964-021-00189-z
19. Jiankun Wang, Qingkai Shen Arc Additively Manufactured 5356 Aluminum Alloy with Cable-Type Welding Wire: Microstructure and Mechanical Properties DOI: https://doi.org/10.1007/s11665-021-05905-y
20. Chengpeng Xue a, Yuxuan Zhang Improving mechanical properties of wire arc additively manufactured AA2196 Al–Li alloy by controlling solidification defects DOI: https://doi.org/10.1016/j.addma.2021.102019
21. Yinghui Zhou Influence of travel speed on microstructure and mechanical properties of wire + arc additively manufactured 2219 aluminum alloy DOI: https://doi.org/10.1016/j.jmst.2019.06.016
22. Van ThaoLe Dinh SiMa Microstructural and mechanical characteristics of 308L stainless steel manufactured by gas metal arc welding-based additive manufacturing DOI: https://doi.org/10.1016/j.matlet.2020.127791
23. A.Rajesh Kannan N.Siva Shanmugam Insight into the microstructural features and corrosion properties of wire arc additive manufactured super duplex stainless steel (ER2594) DOI: https://doi.org/10.1016/j.matlet.2020.127680
24. GuangYang Microstructure and mechanical properties of a novel Cu-reinforced maraging steelfor wire arc additive manufacturing DOI: https://doi.org/10.1016/j.msea.2021.141894
25. Xiaoli Wang Microstructure and Corrosion Properties of Wire Arc Additively Manufactured Multi-Traceand Multilayer StainlessSteel 321 DOI: https://doi.org/10.3390/met12061039
26. Mayank Kumar Singh, Website: www.ijetae.com (ISSN 2250-2459, ISO 9001:2008 Certified Journal, Volume 6, Issue 7, July 2016
27. Han, Q., Gu, Y., Sethi, R., Lacan, F., Johnston, R., Evans, S. L., & Yang, S. (2019). Additive manufacturing of high-strength crack-free Ni-based Hastelloy X superalloy. Additive Manufacturing, 100919. doi: 10.1016/j.addma.2019.100919

How to cite this article: J. Pradeep Kumar, R. Arun Prakash, R. Jaanaki Raman et.al. Wire ARC additive manufacturing of functional metals - a review. *International Journal of Research and Review*. 2023; 10(6): 572-589. DOI: *https://doi.org/10.52403/ijrr.20230671*

******